One-Millipound Mercury Ion Thruster

J. Hyman Jr.,* C. R. Dulgeroff,† S. Kami,‡ and W. S. Williamson§
Hughes Research Laboratories, Malibu, Calif.

A mercury ion thruster has been developed for efficient operation at the nominal 1 mlb (4.45 mN) thrust level with a specific impulse $I_{sp} \cong$ 3000 sec and a total power consumption of $P_T \cong$ 120 W. At a beam voltage $V_B = 1200$ V and beam current $I_B = 72$ mA, the discharge chamber operates with a propellant efficiency (determined from metered beam current alone) $\eta'_{Hg} = 93.8\%$ at an ion-generation energy $\mathcal{E}_I = 276$ eV/ion. Thrust correction due to beam divergence and the presence of doubly-charged mercury ions is -1.7% at a discharge voltage of $V_D = 36$V. The 8 cm diameter thruster advances proven (10,000 hr) component technology to assure the capability for thruster operation over an accumulated beam-on time in excess of 20,000 hr with a capability for 10,000 on-off duty cycles. The system includes a mechanical gimbal system for beam deflection over 10° of azimuth. Discharge-chamber optimization has combined stable current-voltage (I-V) characteristics with high performance efficiency by careful placement of the discharge cathode near the location of a magnetic-field zero just upstream of the thruster endplate. Highest propellant efficiency is achieved when the optical transparency of the accel electrode is reduced to minimize the loss of un-ionized mercury atoms.

Introduction

PROTOTYPE development has been completed of an electron-bombardment mercury ion thruster which operates at a nominal thrust level of 1 mlb (4.45 mN). This program has advanced the technology of satellite-control ion thrusters to accommodate demands imposed by spacecraft mission requirements projected for this decade and beyond. It builds upon experience gained in earlier development of a 5 cm structurally integrated ion thruster (SIT-5) which has been flight qualified for operation at 0.47 mlb (2.09 mN) of thrust.[1] That technology is extended to include applications where higher thrust is required through development of an 8 cm Satellite-Control Ion Thruster (SIT-8).[2,3] The level of component technology has also been advanced to assure the capability for thruster operation for accumulated beam-on times in excess of 20,000 hr with a capability for 10,000 on-off duty cycles. A mechanical thruster-gimbal system has been developed which provides a ±10° vectoring capability in the two dimensions perpendicular to the thruster axis.

Technical Program

The initial goal identified for development of the SIT-8 thruster was to achieve efficient operation at the 1 and 2 mlb thrust levels. To accommodate the maximum thrust requirement, an 8 cm beam diameter was chosen for this development by direct scaling from the Hughes 30 cm thruster which operates at a maximum thrust level of 30 mlb.[4] At maximum thrust level, the beam-extraction system of either thruster would operate at an average beam-current density just below $j_B = 3$ mA/cm; long term operation at higher levels has not yet been demonstrated.

Immediate mission goals have restricted initial optimization of the SIT-8 thruster to the 1 mlb (4.45 mN) thrust level, and special techniques have been developed to ensure high operating efficiency at the lower beam-current value. The NASA-developed Small Hole Accel Grid (SHAG) beam-extraction system has been singularly effective in helping to attain design performance goals.[5] The SHAG system employs a high-transparency screen electrode to minimize discharge power,[6] while high propellant-utilization efficiency is achieved simultaneously with an accel electrode of low optical transparency which limits neutral-particle losses.[5] This combination has been found to be capable of well collimated beam-formation characteristics generating near parallel ion trajectories within a single beamlet. Use of the SHAG system, however, precludes the use of intergrid displacement to achieve beamlet deflection either for the purpose of thrust vectoring[7] or for beam-trajectory compensation,[8,9] since the outermost ion trajectories pass vanishingly close to the sides of the beam-forming apertures.

A thruster gimbaling system has been developed for use with the SIT-8 thruster, which provides ±10° of thrust deflection in the two dimensions perpendicular to the thruster axis. Although all gimbal measurements were carried out with a conventional-accel extraction system, thruster gimbaling is fully compatible with operation of the SIT-8 with the SHAG extraction system.

Thruster Description

An isometric drawing of the SIT-8 thruster is shown in Fig. 1. The discharge chamber of the SIT-8 thruster consists of an outer shell assembly which is formed by rolling thin stainless-steel sheet stock. Structural rigidity of this thin-walled shell is provided by circular stiffening ribs and by flanged sleeves located at the two ends. Axial strength of the structure is provided by rod-shaped permanent magnets mounted axially around the periphery. Magnets are mounted to the flanged sleeves by lugged collars which are swaged onto the ends of the magnets and spot-welded securely to the flanges. These flanges also serve as the interface between the endplate on the closed end of the discharge chamber, and the mount for the beam-extraction system on the opposite end. The thruster endplate and electron baffle are covered with tantalum to control ion-bombardment sputter erosion. An 8.6 cm diam cylindrical anode is supported within the shell by means of insulating support posts which are shielded against sputtering. To avoid potential problems associated with metal-flake formation, a wire-mesh cylinder lines the inner surface of the anode shell.[5] The cathode-cup polepiece is attached to the inner surface of the thruster endplate.

Presented as Paper 75-386 at the AIAA 11th Propulsion Conference, New Orleans, La., March 19-21, 1975; received April 21, 1975; revision received Feb. 23, 1976. This development was funded in part by the NASA Lewis Research Center under NASA Contract NAS 3-15523 (Amendment No. 6), NAS 3-17791, and NAS 3-18917.

Index category: Electric and Advanced Space Propulsion.

*Head of Plasma Research Section, Ion Physics Department. Associate Fellow AIAA.

†Senior Staff Physicist, Ion Physics Department.

‡Staff Engineer, Ion Physics Department.

§Member of Technical Staff, Ion Physics Department. Member AIAA.

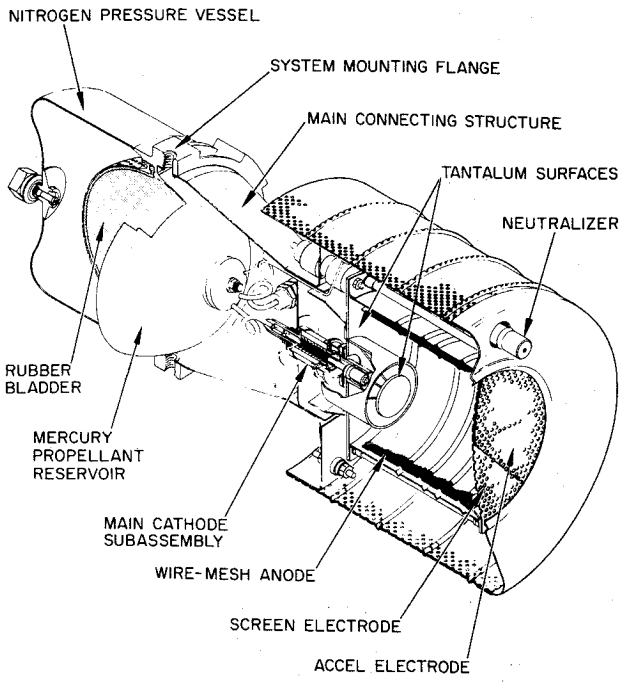

Fig. 1 SIT-8 mercury ion thruster (prototype configuration).

The main cathode subassembly, located on the upstream end of the 8 cm thruster endplate, is essentially the same as that employed successfully with the SIT-5 system. By choosing a vaporizer plug of slightly different shape than that employed in the SIT-5 system, a porous cylinder of the same diameter is capable of supplying the higher value of mercury-vapor flow, which is required for the SIT-8 system.

The neutralizer subassembly follows the SIT-5 design closely, with the single modification being the inclusion of a neutralizer isolator. The neutralizer is mounted so that the cathode axis is directed parallel to the axis of the thruster. An enclosed keeper is used, which is mounted directly to the neutralizer-cathode alignment structure. This mounting structure extends the full length of the thruster ground screen and provides a support for all components of the neutralizer assembly.

A ring of terminals is provided on the ground-screen end-flange for the various electrical connections. Connections between these terminals and the thruster components are made using short lengths of uninsulated tantalum wire. Sputter shielding is employed at both ends of these terminals to ensure that shorting cannot occur across insulating surfaces.

The beam-extraction system is fabricated in a dish-contoured shape to maintain structural rigidity against deformation, even though the electrode elements are of thin cross section. This permits the use of a high-perveance electrode pair, in which the screen-to-accel separation is set to a small value. Without the dished geometry, electrode shorting might occur under operating conditions where thermal gradients would otherwise cause severe deformation. Critical dimensions are listed in Table 1 for the High-Open-Area (HOA) and SHAG beam-extraction systems which have both been tested with the SIT-8 thruster.

No propellant tank was designed or fabricated under the subject program, because the SIT-8 thruster was designed for attachment to the existing SIT-5 tankage system. The propellant tank shown attached to the SIT-8 thruster in Fig. 1 is borrowed from the earlier SIT-5 development. As shown in Fig. 1, system mass is 3 kg including propellant tankage for 6.8 kg of mercury propellant; this is sufficient for 10,000 hr of operation.

Thruster Performance

Thruster performance has been evaluated at the 1-mlb thrust level for operation with both the HOA and SHAG beam-extraction systems. Much higher thruster efficiency is achieved with the SHAG system, because the low-open-area accel electrode greatly restricts the loss of un-ionized mercury propellant. The SHAG system is also distinguished by its capability for prevention of electron backstreaming with very low value of accel voltage.

Discharge-Chamber Performance

Performance curves are shown in Fig. 2 for operation of the prototype model SIT-8 thruster with both the HOA and SHAG beam-extraction systems; the mechanism for the dramatic increase in propellant utilization efficiency achieved by the use of the SHAG system has earlier been explained by Hudson and Banks and is summarized as follows.[5] For a given discharge-chamber operating point, neutral-mercury density inside the discharge chamber has a unique value, as described by Kaufman,[10] which does not depend on external conditions such as the size of apertures in the accel electrode. Therefore, neutral-loss through the beam-extraction system is directly proportional to the open area of the accel electrode. This relationship can be exploited to project performance data from one system design to another. As a case in point, for any given value of ion formation energy, the propellant efficiency η_{Hg} (SHAG) can be projected from HOA performance data in Fig. 2 by the expression

$$\eta'_{Hg}(\text{SHAG}) = \frac{I_B}{I_B + I_{Hg}(\text{HOA})\dfrac{T_{Ac}(\text{SHAG})}{T_{Ac}(\text{HOA})}} \tag{1}$$

where I_{Hg} is the neutral-mercury loss rate and T is the optical transparancy of the accel electrode. The neutral-mercury loss rate is calculated from the measured value of HOA propellant utilization by the following expression

$$I_{Hg} = I_B\left(\frac{1}{\eta'_{Hg}} - 1\right) \tag{2}$$

The projected curve achieves a best fit with experimental data if an average SHAG accel-aperture diameter $d = 0.762$ mm is used (see Table 1); this value corresponds closely to the rms value of the accel apertures in the NASA SHAG extraction system shown in Fig. 3.

Table 1 Dimensions of SIT-8 beam-extraction systems

Grid element	Optical transparency, %	Grid thickness, mm	Aperture diameter, mm	Center-to-center spacing, mm	Electrode separation, mm	Dish radius of curvature, cm	Number of apertures
Screen	67.5	0.406	1.905				
Accel				2.209	0.635	30.00	1190
HOA	47.7	0.508	1.600				
SHAG	10.8	0.508	~0.762				

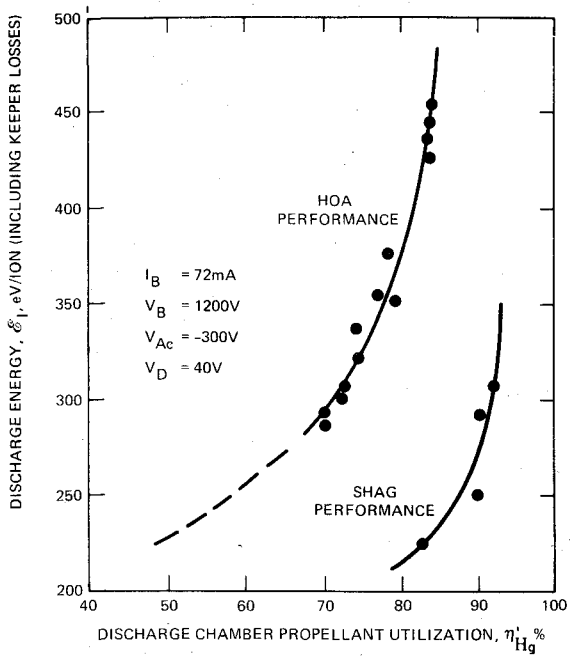

Fig. 2 Effect on SIT-8 performance of beam-extraction system.

SIT-8 thruster performance has been advanced significantly from the level indicated in Fig. 2 by a continuing program of discharge-chamber performance optimization. This program has dealt mainly with the need to combine stable current-voltage (I-V) characteristics with high performance efficiency. In an earlier design, stable operation was facilitated by the use of a variable magnetic baffle which served to shape the magnetic field in the vicinity of the cathode-cup polepiece.[2] By shaping the magnetic field in the annulus separating the main and cathode plasmas, the variable baffle also facilitated ion-beam throttling by adjusting discharge impedance as required to maintain the desired value of beam current.

Since ion-beam throttling was not a goal of the subject development, the variable magnetic baffle has been discarded in order to simplify the SIT-8 prototype configuration shown in Fig. 1. While the prototype configuration is capable of efficient performance, discharge characteristics were initially characterized by high-level oscillations in the discharge current and a tendency toward mode switching to a less efficient operating condition. Stable and efficient discharge-chamber characteristics have been re-established in a present configuration by reducing the length of the discharge chamber from the size shown in Fig. 1 while preserving the axial separation between the screen electrode, the lip of the cathode-cup polepiece, and the cathode tip. These modifications place the cathode tip near the saddle-point-zero of magnetic field which occurs near the plane of the thruster endplate. It is interesting to note that the thruster can be throttled to 0.5 mlb (2.23 mN) in this configuration with stable discharge characteristics. Data are given in Fig. 4 which demonstrate that efficient performance is obtained over the entire thrust range from 0.5 mlb to 1.0 mlb.

Optimal discharge-chamber performance characteristics are given in Table 2 for operation of the SIT-8 thruster at the nominal 1 mlb thrust level in its present configuration. A beam-current value $I_B = 72$ mA was chosen to represent the 1 mlb (4.45 mN) nominal setpoint in order to provide sufficient margin for previously undetermined thrust losses due to beam divergence and the presence of doubly-charged mercury ions; it is seen from Table 2 that this choice was conservative.

Ion Beam Characterization

Thrust losses due to beam divergence and the presence of doubly-charged mercury ions were determined from

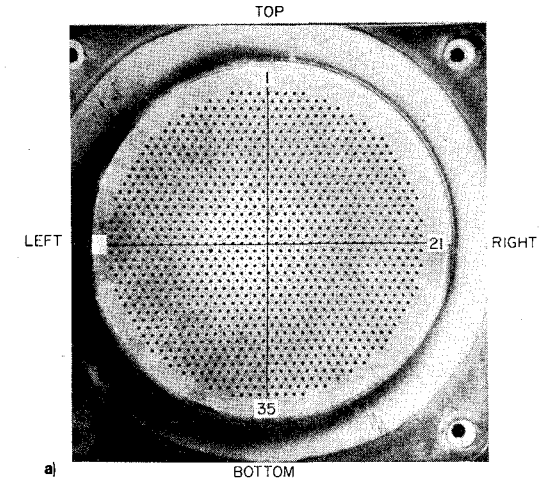

Left to Right	Aperture Number	Top to Bottom
0.061	1	0.061
0.061	2	0.061
0.061	3	0.064
0.061	4	0.057
0.061	5	0.053
0.066	6	0.057
0.074	7	0.061
0.081	8	0.061
0.081	9	0.066
0.084	10	0.066
0.084	11	0.071
0.089	12	0.074
0.084	13	0.079
0.081	14	0.084
0.074	15	0.066
0.071	16	0.084
0.061	17	0.089
0.061	18	0.084
0.061	19	0.084
0.061	20	0.084
0.061	21	0.089
	22	0.089
	23	0.084
	24	0.079
	25	0.079
	26	0.074
	27	0.071
	28	0.066
	29	0.066
	30	0.061
	31	0.061
	32	0.061
	33	0.061
	34	0.061
	35	0.061

b)

Fig. 3 NASA SHAG accel electrode: a) photo; b) sample accel aperture diameters.

measurements obtained with an ExB-type current density and velocity analyzer mounted 50 cm downstream of the SHAG beam-extraction system.¶ The analyzer has high angular resolution and is capable of articulation and translation across the beam.[11] The results of these measurements are given in Fig. 5, where a profile of the SIT-8 ion beam is presented as a function of angle from the thruster axis. (In this form of presentation, the thruster is taken to be a point source.) The data points shown in this figure are well approximated by a gaussian normal curve with a full width at half maximum of 17°. The thrust loss due to beam divergence is calculated to be 0.8%.

The measured ratio of the doubly-charged ion current to the singly-charged ion current is plotted in Fig. 6 as a function of discharge voltage; for an operating voltage of $V_D = 36$ V, the reduction in calculated thrust due to the presence of doubly-charged ions in the beam is 0.9%. The reduction in the metered value of propellant utilization efficiency is plotted in Fig. 7, also as a function of discharge voltage.

¶Since the electrodes which comprise the SHAG extraction system are spherically dished, the beamlet trajectories tend to follow lines that converge to the center of curvature of the extraction electrodes. This point is located 30 cm downstream of the beam-extraction system (see Table 1).

Table 2 Optimal SIT-8 performance (SHAG beam-extraction system)

Performance Parameter	Setpoints	Power Distribution
Thrust,[a] mN	5.04	
Specific impulse,[a] sec	2926	
Total input power, W	122.09	
Total efficiency,[a] %	61.3	
Electrical efficiency, %	72.0	
Total utilization,[a] %	85.2	
Discharge utilization,[a] %	91.8	
Total neutral flow, mA	83.25	
Power/thrust,[a] W/mN	24.22	
eV/ion excluding keeper,[b] V	275	
eV/ion including keeper,[b] V	278	
Beam current, I_B, mA	72	
Beam voltage, V_B, V	1220	
Output beam power, W		87.84
Accelerator voltage, V_{Ac}, V	-300	
Accelerator drain current, I_{Ac}, mA	0.30	
Accelerator drain power, W		0.09
Neutralizer coupling potential, V_C, V	-20	
Neutralizer coupling current, I_C, mA	72	
Neutralizer coupling power, W		1.44
Discharge voltage, V_D, V	36	
Discharge current, I_D, A	0.550	
Discharge power, W		19.80
Cathode:		
Keeper voltage, V_{MK}, V	7.5	
Keeper current, I_{MK}, A	0.030	
Keeper power, W		0.23
Heater voltage, V_{MCH}, V	0.0	
Heater current, I_{MCH}, A	0.0	
Heater power, W		0
Vaporizer voltage, V_{MV}, V	4.0	
Vaporizer current, I_{MV}, A	1.4	
Vaporizer power, W		5.6
Flowrate, mA	77.25	
Neutralizer:		
Keeper voltage, V_{NK}, V	14	
Keeper current, I_{NK}, A	0.35	
Keeper power, W		4.9
Heater voltage, V_{NCH}, V	0.0	
Heater current, I_{NCH}, A	0.0	
Heater power, W		0
Vaporizer voltage, V_{NV}, V	2.3	
Vaporizer current, I_{NV}, A	0.95	
Vaporizer power, W		2.19
Flowrate, mA	6.0	
Total Power		122.09

[a] These values are corrected for neutralizer floating potential, beam divergence, and the presence of doubly-charged mercury ions.

[b] Computed using meter beam current.

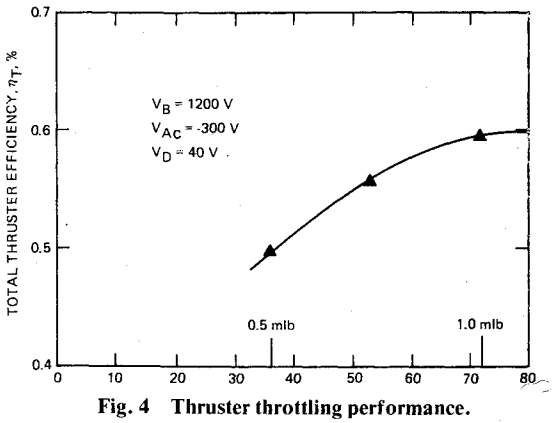

Fig. 4 Thruster throttling performance.

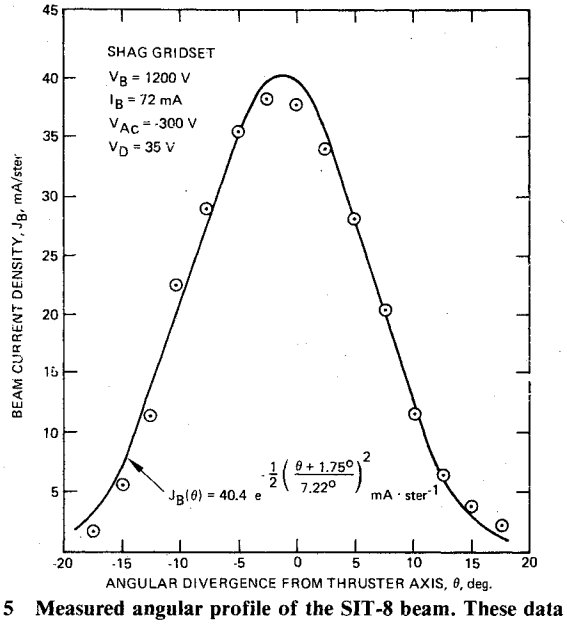

Fig. 5 Measured angular profile of the SIT-8 beam. These data are presented in a form which assumes the thruster to be a point source. The beam intensity reaches 10% of its peak value at a half-angle of 15°. A gaussian normal curve (obtained by a least-squares curve-fitting technique) is shown for comparison.

Beam-Handling Capabilities

The beam-transport capability of the SHAG beam-extraction system was evaluated by varying the total accelerating voltage $V_T = |V_B| + |V_{Ac}|$ while maintaining a constant ratio of beam voltage to total accelerating voltage, $V_B/V_T = 0.8 = \text{constant}$. Variations in beam and accel currents are presented in Fig. 8. Direct accel interception results if total accelerating voltage is reduced below ($V_T \lesssim 1000$ V); this defines the limiting beam-handling capability of the 8 cm SHAG grid set. The beam-current variation with accelerating voltage reflects a change in mercury-propellant flowrate which was automatically controlled to hold the discharge voltage constant.

Below a total acceleration voltage $V_T < 400$ V, there is an apparent increase in beam current which actually is the result of electron-current backstreaming from the beam plasma to the discharge plasma. The onset of electron backstreaming is shown in Fig. 9, where the increase in apparent ion-beam current is plotted as a function of accel voltage (while beam voltage is held near its nominal value $V_B = 1200$ V). For the HOA extraction system, electron backstreaming approaches zero at the nominal value of accel voltage $V_{Ac} = -300$ V, but increases as the magnitude of accel voltage is reduced from that value. As shown in Fig. 9, the SHAG extraction system is

Table 3 Gimbal system specification

Gimbaling power requirements[a] (each axis)	2.4 W (12 V dc, 0.2 A for each motor)
Time response of gimbal drive system (-10° to +10°)	1 min
Gimbal system mass	1.23 kg
Gimbal system driving force – H-axis, V-axis (on motor in line with worm gear)	24.5 N, 16.7 N
Distance between the gimbaled center-of-mass and center-of-rotation	6.7 cm

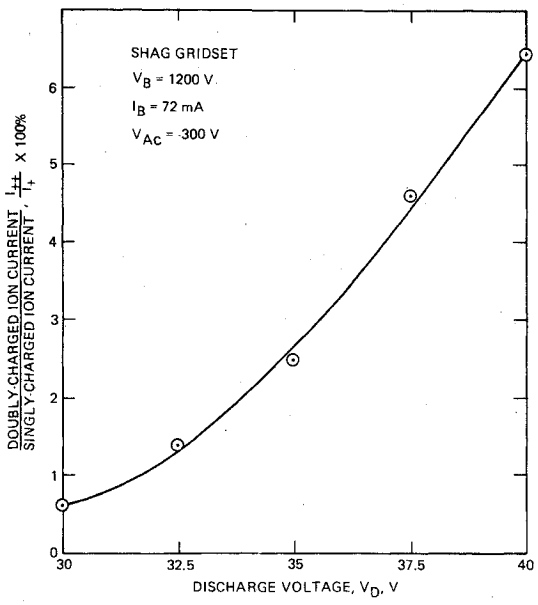

Fig. 6 Doubly-charged mercury ion fraction for total SIT-8 beam.

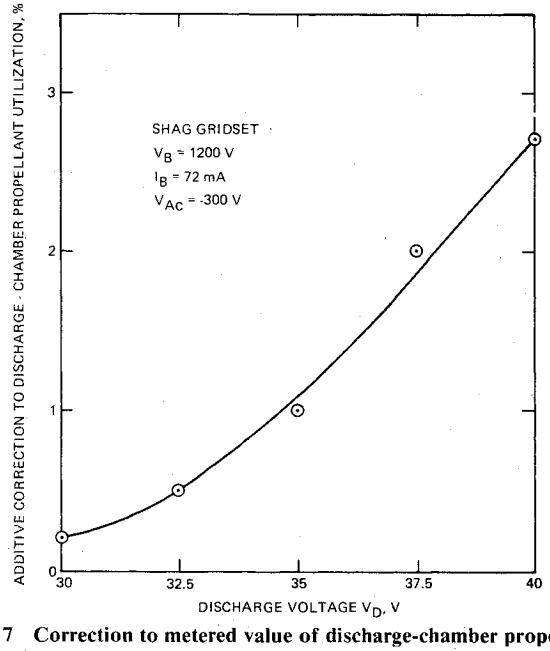

Fig. 7 Correction to metered value of discharge-chamber propellant utilization.

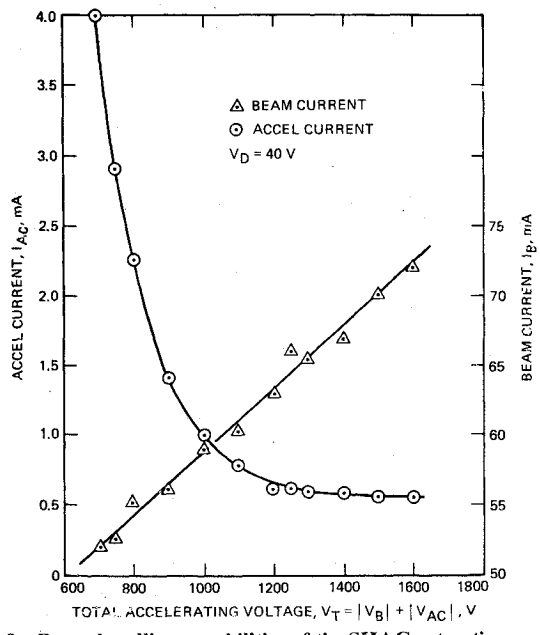

Fig. 8 Beam-handling capabilities of the SHAG extraction system.

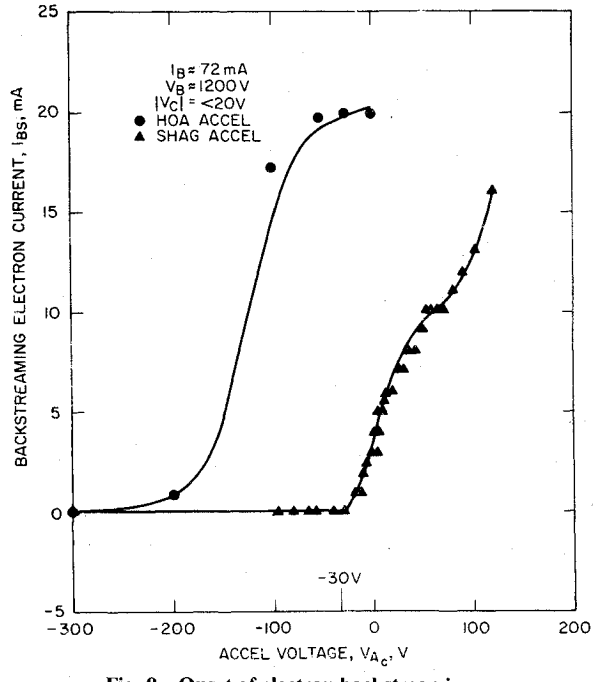

Fig. 9 Onset of electron backstreaming.

effective in preventing electron backstreaming at a greatly reduced magnitude of accel voltage, $V_{Ac} = -30$ V. The SHAG system has a lower backstreaming limit because the accel apertures are of a size which is comparable with accel-electrode thickness. In this configuration, electric-field penetration of the beam-forming apertures is minimized, and the potential imposed at the centerline of the accel-electrode beam-forming apertures approaches the potential applied to the electrode itself.

Thruster Gimbal System

A Thruster Gimbal System was developed under the SIT-8 thruster program which achieves thrust deflection by gimbaling the entire thruster (not including propellant tankage) about two orthogonal axes perpendicular to the thruster axis.

Gimbal Design

A plan view of the thruster gimbal system is shown in Fig. 10. In this design, the ground-screen endflange is bolted to a central circular ring at eight locations. The ring in turn is supported from shafts projecting from the center races of two sets of ball bearings. The outer races are connected to a circular yoke which is itself supported at the two orthogonal locations by a similar pair of bearings supported by the mounting flanges of the gimbal system. Both gimbal rings are fabricated of Type 6061 aluminum. The inner ring has a mass of 0.070 kg and the outer ring has a mass of 0.170 kg. The mass of the gimbaled thruster is 1.4 kg while the mass of the gimbaling system itself is 1.23 kg. Other specifications of the gimbal system are listed in Table 3. Ball-bearing pivots have been lubricated for high-temperature space applications by sputter deposition of a MoS^2 film using a process described by Talivaldis Spalvins of LeRC.[12]

A linear actuator, supported from one of the two mounting flanges, is used to tilt the thruster flange about the two outermost bearing sets. A second linear actuator, mounted directly from the circular outer yoke, is used to tilt the thruster flange

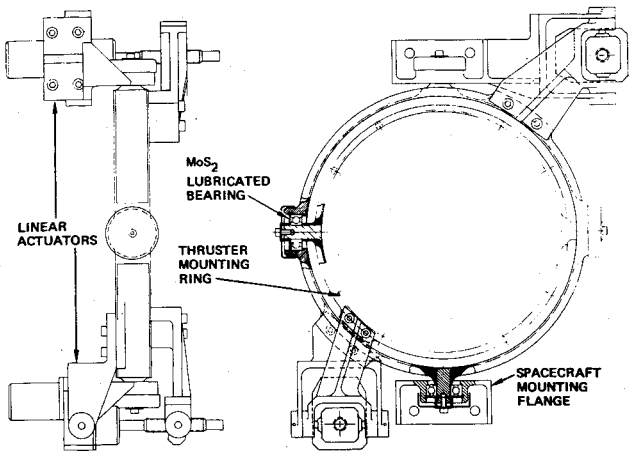

Fig. 10 Thruster gimbal system.

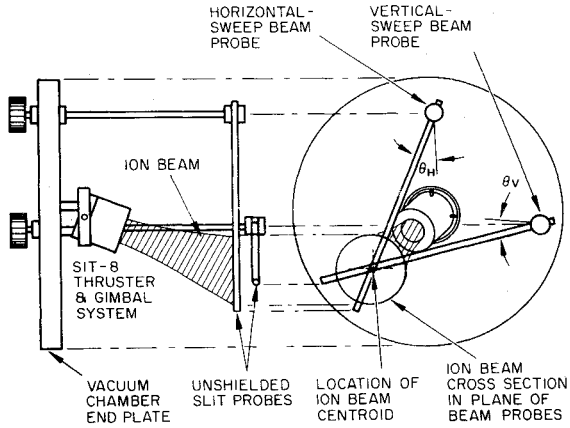

Fig. 11 Beam probe configuration.

about the axis of the two innermost bearing sets. The linear actuators are adapted from an existing flight-qualified device which was developed by the Hughes Space and Communication Group for use as an Intelsat IV antenna positioner.

Beam Vector Measurements

The thruster gimbaling system was evaluated by measuring the change in ion-beam thrust vector as a function of actuator-motor step number. For this evaluation, the SIT-8 thruster was attached to the gimbal system, which was mounted on a vacuum-chamber endflange. Beam vector measurements were made at a beam voltage $V_B = 1200$ V and a beam current $I_B = 72$ mA. All beam-deflection measurements were performed in a 1.2 m diameter vacuum chamber at a pressure of less than 4×10^{-6} Torr. The stepper motors responded as expected and reached an operating temperature of +90°C, well within the operating range for the stepper motor (-65°C to +125°C). The temperature of the gimbal-system mount nearest to the thruster reached +60°C. Two probes were used to measure the current-density contours required to establish the centroid of the thrust vector. The probes consist of 36 cm long, 0.64 cm diameter stainless-steel tubes which are swept about orthogonal axes across the ion beam. Figure 11 shows how these probes are oriented with respect to the beam. The probes were located about 47 cm from the face of the thruster. At this distance, a beam vector angle of 1° results in a linear displacement of 0.82 cm. The centroid location was determined by the intersection of the angular measurements for maximum intensity of each probe. The intensities for each probe were recorded as a function of angle on an *X-Y* recorder; a typical plot of zero deflection is shown in Fig. 12a). A plot for horizontal-axis deflection of 5°

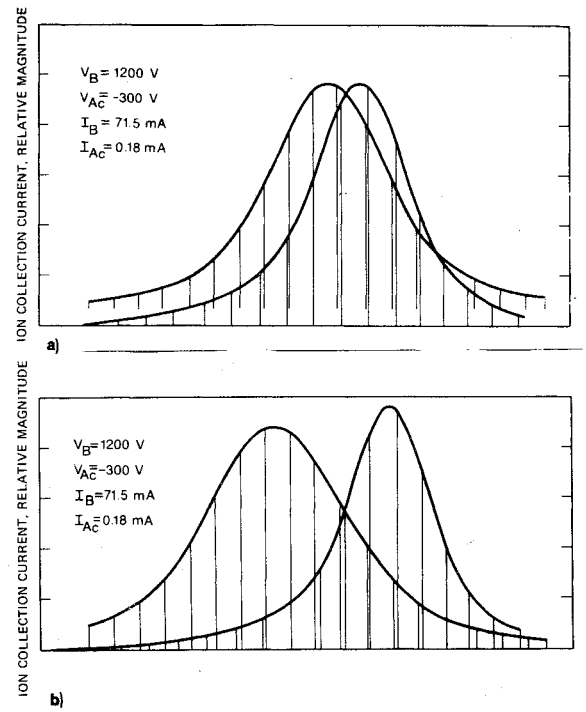

Fig. 12 a) Beam profile measurements. Beam scans for zero deflection. b) Beam scans for 5° horizontal-axis deflection.

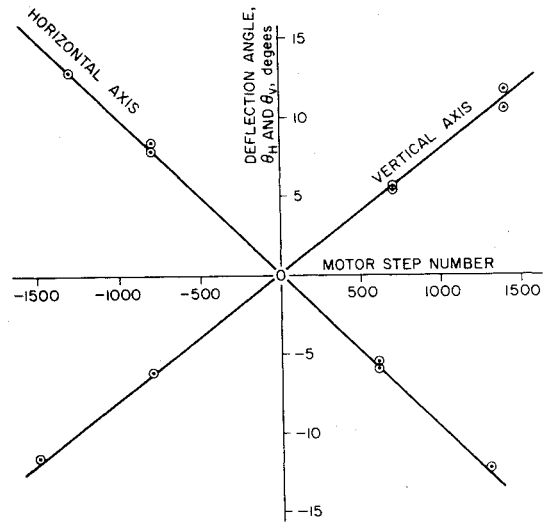

Fig. 13 Beam deflection characteristics.

is shown in Fig. 12b). Data are presented in Fig. 13 which show the position of the beam centroid as a function of actuator-motor step number. These data are linear and repeatable within a standard deviation of 1°.

Summary of Results

An 8 cm Satellite-control Ion Thruster (SIT-8) has been developed which extends the technology established in development of the SIT-5 thruster to include applications where a higher thrust level is required, and which advances the level of component technology to assure the capability for thruster operation for accumulated beam-on times of 20,000 hr with a capability for 10,000 on-off duty cycles. Discharge-chamber optimization has produced highly stable operation over a wide range of operating parameters, with high discharge-chamber propellant utilization ($\eta'_{Hg} = 93.2\%$ as determined from metered beam current alone) and low power losses ($\varepsilon_I = 276$ *eV*/Ion). Thrust corrections due to beam

divergence and the presence of doubly-charged mercury ions have been measured and found to total -1.7%. A thruster gimbal system has been developed which provides an attractive approach to beam-vectoring requirements; the thruster gimbal system provides a measured capability for thrust deflection of 10° in two orthogonal directions perpendicular to the thruster axis.

References

[1] Hyman Jr., J., "Development of a 5-cm Flight-Qualified Mercury Ion Thruster," *Journal of Spacecraft and Rockets*, Vol. 10, Aug. 1973, pp. 503-509.

[2] Hyman Jr., J. and Poeschel, R. L., "Satellite Control Mercury Ion Thruster," AIAA Paper 73-1132, Lake Tahoe, Nev., 1973.

[3] Hyman Jr., J., "8 cm Technology Thruster Development," Final Report, NASA Contract NAS 3-17791, NASA CR-134685, Hughes Research Laboratories, Malibu, Calif., July 1974.

[4] King, H. L. and Poeschel, R. L., "A 30 cm Ion Thruster Module," *Journal of Spacecraft and Rockets*, Vol. 8, April 1971, pp. 420-423.

[5] Banks, B. A., "Eight cm Mercury Ion Thruster System Technology," AIAA Paper 74-1116, San Diego, Calif., 1974.

[6] Knauer, W., "Power Efficiency Limits of Kaufman Thruster Discharges," AIAA Paper 70-177, New York, N. Y., 1970.

[7] Collett, C., King, H. L., and Schnelker, D., "Vectoring of the Beam from Ion-Bombardment Thrusters," AIAA Paper 71-691, Salt Lake City, Utah, 1971.

[8] Seliger, R. L., Nudd, G. R., Brewer, G. R., and Amboss, K., "Analysis of the Expected Thrust Misalignment of Kaufman Thrusters," *Journal of Spacecraft and Rockets*, Vol. 7, April 1970, pp. 422-428.

[9] Potosky, J., "Compensation of Dished Grid Ion Optics," Hughes Aircraft Company IDC, Malibu, Calif., Org. 30-26, Dec. 1972.

[10] Kaufman, H. R., "Ion Thruster Propellant Utilization," Ph.D. Thesis, Department of Mechanical Engineering, Colorado State University, Fort Collins, Col.

[11] Vahrenkamp, R. P., "Measurement of Doubly Charged Ions in the Beam of 30 cm Mercury Bombardment Thruster," AIAA Paper 73-1057, Lake Tahoe, Nevada, 1973.

[12] Spalvins, T., "Lubrication with Sputtered MoS_2 Films," *ASLE Transactions*, Vol. 14, 1971, p. 267.